MHD Flow And Radiative Heat Transfer Of Micropolar Dusty Fluid Suspended With Alumina Nanoparticles Over A Stretching Sheet Embedded In A Porous Medium

Dr. Krishnamurthy M. R.
Department of Mathematics, JNN College of Engineering,
Shimoga-577204
kittysa.mr@gmail.com

ABSTRACT:

This article aims to study the boundary layer flow and heat transfer of an incompressible Al_2O_3-water nanoparticle on Micropolar fluid with homogeneously suspended dust particles in the presence of thermal radiation. The flow is generated due to linear stretching surface in the presence of uniform magnetic field. The similarity transformations are used to reduce the governing partial differential equations into a set of non-linear ordinary differential equations. Numerical solutions are obtained for these equations using efficient numerical technique Runge-Kutta-Fehlberg fourth-fifth order method with the help of symbolic algebra software MAPLE. Numerical values of velocity and heat transfer co-efficient are plotted in the form of graphs for different flow controlling parameters. The comparison of the present results with the existing numerical solutions in a liming sense is also shown and this comparison is very good.

Keywords: Boundary layer flow, heat transfer, dust particles, nanoparticles, micropolar fluid, thermal radiation.

1. INTRODUCTION

From a technological point of view, the study of flow driven by a moving surface in otherwise quiescent fluid has attracted considerable practical interest. Such a system is used in a wide variety of manufacturing processes such as glass fiber drawing, crystal growing, plastic extrusion, continuous casting, etc. Sakiadis [1] initiated the theoretical analysis for a new class of boundary-layer problems, with solutions substantially different from those for boundary layer flow on surfaces of finite length. Further, he has examined the boundary-layer behavior on continuous surfaces and derived the basic differential and integral momentum equations of boundary-layer theory for such surfaces. Later, Tsou et al. [2] showed experimentally that such a flow is physically realizable. Therefore, many related analytical and numerical solutions have been obtained for different aspects of this class of boundary layer problems.

The problem of steady two-dimensional boundary layer flow of an incompressible and viscous fluid caused by a stretching sheet, whose velocity varies linearly with the distance from a fixed point on the sheet seems to be first studied by Crane [3]. It should be mentioned that the problem of flow due to a stretching sheet belongs to an important class of exact solutions of the Navier-Stokes equations. Watanabe and Pop [4] investigated the heat transfer in thermal boundary layers of MHD Newtonian/non-Newtonian flows over a flat plate. Chakrabarti and Gupta [5] have discussed the MHD flow and heat transfer over a stretching sheet. Further Grubka and Bobba [6] analyzed heat transfer studies by considering the power-law variation of surface temperature. Chen [7] studied the mixed convection of a power law fluid past a stretching surface in the presence of thermal radiation and magnetic field. Abel et al. [8] have extended to study the effects of magnetic field on viscoelastic fluid flow and heat transfer over a stretching sheet with internal heat generation/absorption. The heat transfer aspects of similar problems were studied by Dutta et al. [9],

Ali [10], Vajravelu and Roper [11] and many others.

The theory of micropolar fluid was first introduced by Eringen [12] in the late 19th century. This theory has a wide range of applications in fluid mechanics and other related areas, in which coupling between the spin of each particle and microscopic velocity is taken into account. Boundary layer theory for micropolar fluid was first introduced by Peddison et al. [13]. Numerical analysis of micropolar fluids towards a stretching sheet is given by Nazar et al. [14]. Rahman and Sattar [15] reported transient convective heat transfer flow of a micropolar fluid past a continuously moving vertical porous plate with time dependent suction in the presence of radiation. Rapits [16] presented the solution to the flow of a micropolar fluid past a continuously moving plate in the presence of thermal radiation. Ishak [17] studied the thermal boundary layer flow over stretching sheet in a micropolar fluid with radiation effect. Turkyilmazoglu [18] investigated the micropolar fluid flow due to a permeable stretching sheet. A second order slip flow and magnetic field on boundary layer flow of micropolar fluid past a stretching sheet has been examined by Ibrahim [19].

It is well known that conventional heat transfer fluids, including oil, water, and ethylene glycol mixture are poor heat transfer fluids, Thermal conductivity of these fluids plays an important role on the heat transfer coefficient between the heat transfer medium and the surface. An innovative technique for improving heat transfer by using ultra fine solid particles in the fluids has been used extensively during the last several years. Nanofluid, a term introduced by Choi [20], is a base fluid with suspended metallic nano-scale particles called nanoparticles. The characteristic feature of nanofluids is its thermal conductivity enhancement, a phenomenon observed by Masuda et al. [21]. Buongiorno [22] observed the abnormal increase of the thermal conductivity of nanofluids in his comprehensive survey on convective transport in nanofluids. Xuan et al. [23] have examined the transport properties of nanofluid and have expressed that thermal dispersion, which takes place due to the random movement of particles, takes a major role in increasing the heat transfer rate between the fluid and the wall. Das et al. [24] have shown that the thermal conductivity for nanofluid increases with increasing temperature. They have also observed the stability of Al_2O_3- water and $CuO-$ water nanofluid. The viscosity of the nanofluid increases rapidly with inclusion of nanoparticles. Rashidi et al. [25] discussed the buoyancy effect on MHDflow of nanofluid over a stretching sheet in the presence of thermal radiation. The model of nanofluid flow and heat transfer over a moving surface with variable thickness in the presence of Brownian motion, thermophoresis, chemical reaction, heat generation, and thermal radiation have been illustrated by Madaki et al [26]. Prasannakumara et al. [27] considered the steady flow, heat and mass transfer of an incompressible Jeffrey nanofluid over a horizontal stretching surface.

All the above mentioned investigations are restricted to only pure fluid problems. In nature, the fluid in pure form is rarely available. Air and water contains impurities like dust particles and foreign bodies. Therefore the studies of two-phase flows in which solid spherical particles are distributed in a clean fluid find practical applications like petroleum industry, purification of crude oil, and physiological flows. Other important applications involving dust particles in boundary layers include soil salvation by natural winds, lunar surface erosion by the exhaust of a landing vehicle and dust entrainment in a cloud formed during a nuclear explosion. Saffman [28] has formulated the equations for this fluid and has discussed the stability of the laminar flow of a fluid in which the dust particles

are uniformly distributed. Chakrabarti [29] analyzed the boundary layer flow of dusty gas. Datta and Mishra [30] have investigated boundary layer flow of a dusty fluid over a semi infinite flat plate. Evgeny and Sergei [31] discussed the stability of the laminar boundary layer flow of dusty gas on a flat plate. Vajravelu and Nayfeh [32] analyzed the hydromagnetic flow of dusty fluid over a stretching sheet with the effect of suction. Ezzat [33] critically examined the space approach to the hydro-magnetic flow of a dusty fluid through a porous medium. Krishnamurthy et al. [34] studied the effect of nonlinear thermal radiation on slip flow and melting heat transfer of dusty fluid suspended with Cu nanoparticles

immersed in a porous medium over a stretching sheet.

Encouraged by the above literature survey, we intended to investigate the boundary layer flow and heat transfer of Al_2O_3-water nanoparticle on micropolar fluid over a stretching sheet embedded with dust particles in the presence of thermal radiation. The governing nonlinear partial differential equations along with the boundary conditions are reduced into a dimensionless form and then are solved numerically using fourth-order Runge-Kutta method with the help of algebraic software Maple.

Table 1: Thermo physical properties of water and nanoparticles.

	$\rho(kg/m^3)$	$C_p(j/kgk)$	$k(W/mk)$
Pure water (H_2O)	997.1	4179	0.613
Aluminium Oxide (Al_2O_3)	3970	765.0	40.000

2. MATHEMATICAL FORMULATION AND SOLUTION OF THE PROBLEM

Consider a steady, two-dimensional, laminar, boundary layer flow of an dusty nano micropolar fluid over a stretching sheet coinciding with the plane $y = 0$ and the flow being confined to $y > 0$. The flow is generated, due to the linear stretching of the sheet, caused by the simultaneous application of two equal and opposite forces along the x-axis. Keeping the origin fixed, the sheet is then stretched with a velocity $U_w(x) = bx$, where b is constant. Further the flow field is exposed to the influence of an external transverse magnetic field of strength B_0(along y-axis) as shown in figure 1. The dust particles are assumed to be uniform in size and number density of the dust particle is taken as a constant throughout the flow.

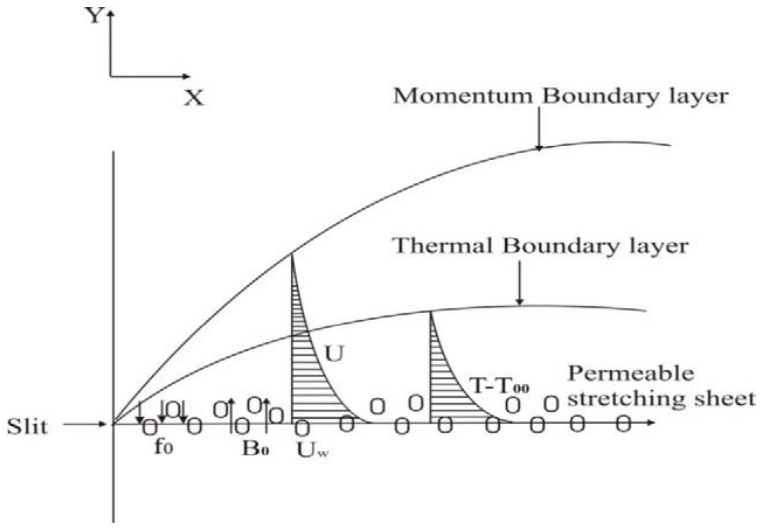

Figure 1: Schematic representation of boundary layer flow.

Under the above assumption, the basic two-dimensional boundary layer equations are as Follows,

$$\frac{\partial u}{\partial x}+\frac{\partial v}{\partial y}=0, \tag{2.1}$$

$$u\frac{\partial u}{\partial x}+v\frac{\partial u}{\partial y}=\left(\nu_{nf}+\frac{k}{\rho_{nf}}\right)\frac{\partial^2 u}{\partial y^2}+\frac{KS}{\rho_{nf}}\left(u_p-u\right)+\frac{k}{\rho_{nf}}\frac{\partial N}{\partial y}-\frac{\sigma {B^2}_0}{\rho_{nf}}u-\frac{\nu_{nf}}{k'}u, \tag{2.2}$$

$$u\frac{\partial N}{\partial x}+v\frac{\partial N}{\partial y}=\frac{\gamma}{\rho_{nf}j}\frac{\partial^2 N}{\partial y^2}-\frac{k}{\rho_{nf}j}\left(2N+\frac{\partial u}{\partial y}\right), \tag{2.3}$$

$$\frac{\partial u_p}{\partial x}+\frac{\partial v_p}{\partial y}=0, \tag{2.4}$$

$$\rho_p\left(u_p\frac{\partial u_p}{\partial x}+v_p\frac{\partial u_p}{\partial y}\right)=KS\left(u-u_p\right), \tag{2.5}$$

Where (u,v) and (u_p,v_p) are the velocity components of nanofluid and dust phases along x and y directions, respectively. $K=6\pi\mu_f a$is called Stokes drag constant,$\rho_p=rS$ is the density of dust particles, S is the number density of the dust particles, r is the mass of the dust particle, N is the microrotation or angular velocity whose direction of rotation is normal to the $x-y$plane,ν_{nf} is the kinematic viscosity of the nanofluid, ρ_{nf} is the effective density of the nanofluid and is defined by,$\rho_{nf}=(1-\phi)\rho_f+\rho_s$. Here, ϕ is the solid volume fraction, μ_f is the dynamic viscosity of the base fluid, ρ_f and ρ_s are the densities of the base fluid and nanoparticle, respectively.

j,γ and k are the micro inertia per unit mass, spin gradient viscosity and vertex viscosity respectively, σ is the electrical conductivity, B_0 is uniform magnetic field strength and $k'$is the permeability of the porous medium.

As it was shown by Ahmadi [35], spin-gradient viscosity γ can be defined as

$$\gamma=\left(\mu_{nf}+\frac{k}{2}\right)j=\mu_{nf}\left(1+\frac{R}{2}\right), \tag{2.6}$$

Where μ_{nf} is the dynamic viscosity of the nanofluid and is given by Brickman [36] as, $\mu_{nf}=\frac{\mu_f}{(1-\phi)^{2.5}}.R=\frac{k}{\mu_{nf}}$ is the dimensionless viscosity ratio and is called the material parameter and we take $j=\frac{\nu_{nf}}{a}$as a reference length. This assumption is invoked to allow the field of equations to predict the correct behavior in the limiting case when the micro structure effects become negligible and the total spin N reduces to the angular velocity.

The boundary conditions are,

$$u=U_w(x),\ v=V_w(x),\ \ N=-n\frac{\partial u}{\partial y} \quad \text{at } y=o,$$

$$u=v=0,\ u_p\to 0,\ v_p\to v,\ N\to 0 \quad \text{as } y\to\infty. \tag{2.7}$$

The governing equations (2.1)-(2.5) subject to the boundary conditions (2.7) can be expressed in a simpler form by introducing the following transformations:

$$\eta=\left(\frac{U_w(x)}{\nu_f x}\right)^{1/2}y,\ \ \psi=\left(\nu_f x U_w(x)\right)^{\frac{1}{2}}f(\eta),\quad N=U_w(x)\left(\frac{U_w x}{\nu_f x}\right)^{\frac{1}{2}}h(\eta), \tag{2.8}$$

Where $U_w(x)=bx$ is the stretching sheet velocity, $b>0$ is the stretching rate, $V_w(x)=-f_0\sqrt{b\nu_f}$ is the suction velocity, η is the similarity variable and ψ is the stream function defined in the usual way as $u=\frac{\partial\psi}{\partial y}$and $v=-\frac{\partial\psi}{\partial x}$ and similarly u_p and v_p also, which identically satisfies equations (2.1) and (2.4).

The transformed ordinary differential equations are,

$$(1+R)f''' + (1-\phi)^{2.5}\left[(1-\phi) + \phi\frac{\rho_s}{\rho_f}\right](ff'' - (f')^2) + (1-\phi)^{2.5}[l\beta(F'-f') - Mf'] + Rh' - K_p f' = 0, \quad (2.9)$$

$$\left(1+\frac{R}{2}\right)h'' + (1-\phi)^{2.5}\left[(1-\phi) + \phi\frac{\rho_s}{\rho_f}\right](fh' - f'h) - R(2h+f'') = 0, \quad (2.10)$$

$$FF'' - [F']^2 + \beta[f'-F'] = 0, \quad (2.11)$$

where prime denotes differentiation with respect to η, $l = \frac{rS}{\rho_f}$ is the mass concentration, $\tau_v = r/K$ is the relaxation time of the particle phase, $\beta = 1/b\tau_v$ is the fluid particle interaction parameter for velocity, $M = \frac{\sigma {B^2}_0}{\rho_f b}$ is the magnetic parameter and $K_p = \frac{\nu_f}{bk'}$ is the permeability parameter.

The boundary condition defined as in (2.6) will take the following form,

$$f'(\eta) = 1,\ f(\eta) = f_0,\ h(\eta) = -mf''(0) \text{ at } \eta = 0,$$
$$f'(\eta) = 0,\ F'(\eta) = 0,\ F(\eta) = f(\eta),\ h(\eta) = 0 \text{ as } \eta \to \infty. \quad (2.12)$$

3. HEAT TRANSFER ANALYSIS

The governing boundary layer heat transport equations for both nanofluid with dust particles are given by,

$$(\rho C_p)_{nf}\left[u\frac{\partial T}{\partial x} + v\frac{\partial T}{\partial y}\right] = k_{nf}\frac{\partial^2 T}{\partial y^2} + \frac{\rho_p C_{Pf}}{\tau_T}(T_p - T) + \frac{\rho_p}{\tau_v}(u_p - u)^2 + \mu_{nf}\left(\frac{\partial u}{\partial y}\right)^2 - \frac{1}{(\rho C_p)_{nf}}\frac{\partial q_r}{\partial y}, \quad (3.1)$$

$$(\rho_p C_{mf})\left[u_p\frac{\partial T_p}{\partial x} + v_p\frac{\partial T_p}{\partial y}\right] = -\frac{\rho_p C_{pf}}{\tau_T}(T_p - T), \quad (3.2)$$

where T and T_p are the temperatures of the nanofluid and dust particles, C_{pf} and C_{mf} are the specific heat of nanofluid and dust particles, τ_T is the thermal equilibrium time i.e., the time required by a dust cloud to adjust its temperature to the nanofluid, τ_v is the relaxation time of the dust particle, k_{nf} is the thermal conductivity and $(\rho C_p)_{nf}$ is the heat capacitance of the nanofluid, which are defined as Maxwell [37],

$$(\rho C_p)_{nf} = (1-\phi)(\rho C_p)_f + \phi(\rho C_p)_s,$$
$$\frac{k_{nf}}{k_f} = \frac{k_s + 2k_f - 2\phi(k_f - k_s)}{k_s + 2k_f + 2\phi(k_f - k_s)}, \quad (3.3)$$

Here, k_f and k_s are the thermal conductivities of the base fluid and nanoparticle, respectively. Using the Rosseland approximation for radiation, the radiative heat flux is simplified as,

$$q_r = -\frac{4\sigma^*}{3k^*}\frac{\partial T^4}{\partial y}, \quad (3.4)$$

Where σ^* and k^* are the Stefan-Boltzmann constant and the mean absorption coefficient respectively. The temperature differences within the flow are assumed to be sufficiently small so that T^4 may be expressed as a linear function of temperature T using a truncated Taylor series about the free stream temperature T_∞ and neglecting the higher order terms, we get,

$$T^4 \approx 4T{T^3}_\infty - 3{T^3}_\infty, \quad (3.5)$$

Using (3.4) and (3.5), equation (3.1) reduces to,

$$(\rho C_p)_{nf}\left[u\frac{\partial T}{\partial x} + v\frac{\partial T}{\partial y}\right] = k_{nf}\left(\frac{16\sigma^* {T^3}_\infty}{3k^* k_{nf}}\right)\frac{\partial^2 T}{\partial y^2} + \frac{\rho_p C_{Pf}}{\tau_T}(T_p - T) + \frac{\rho_p}{\tau_v}(u_p - u)^2 + \mu_{nf}\left(\frac{\partial u}{\partial y}\right)^2, \quad (3.6)$$

The solution of (3.3) and (3.6) depends on the nature of the prescribed boundary conditions. We employ two types of heating process as follows.

The prescribed boundary conditions are defined as follows,

$$T = T_w = T_\infty + A\left(\frac{x}{l}\right)^2 \quad \text{(PST case)},$$
$$-k\frac{\partial T}{\partial y} = q_w = D\left(\frac{x}{l}\right)^2 \text{ (PHF case)} \quad \text{at } y = o,$$
$$T \to T_\infty,\ T_p \to T_\infty \text{ as } y \to \infty.$$

(3.7)

Where T_w and T_∞ denote the temperature at the wall and at large distance from the wall respectively. A is a positive constant, which depends on the properties of the fluid and l is the characteristic length and is given by $l = \frac{\sqrt{\nu_f}}{b}$.

Defining the non-dimensional nanofluid phase temperature $\theta(\eta)$ and dust phase temperature $\theta_p(\eta)$ as,

$$\theta(\eta) = \frac{T-T_\infty}{T_w-T_\infty} \text{ and } \theta_p(\eta) = \frac{T_p-T_\infty}{T_w-T_\infty},$$

(3.8)

where $T - T_\infty = A\left(\frac{x}{l}\right)^2 \theta(\eta)$ (PST case)

$T_w - T_\infty = \frac{D}{t}\left(\frac{x}{l}\right)^2 \frac{\sqrt{\nu_f}}{b}$ (PHF case).

Using (2.8), (3.3) and (3.8) into (3.2) and (3.6), we obtain

$$\frac{k_{nf}}{k_f}\left(1+\frac{4}{3}Nr\right)\theta'' + \Pr\left[(1-\phi)+\phi\frac{(\rho C_p)_s}{(\rho C_p)_f}\right](f\theta' - 2f'\theta) + Prl\beta_T[\theta_p - \theta] + PrlEc\beta[F' - f']^2 + PrEcf''^2 = 0,$$

(3.9)

$$F\theta'_p - 2F'\theta_p + \gamma\beta_T[\theta - \theta_p] = 0,$$

(3.10)

where $Pr = \frac{(\mu C_p)_f}{k_f}$ is the Prandtl number, $Ec = \frac{b^2 l^2}{AC_{pf}}$ (PST case) and $Ec = \frac{b^2 l^2 t}{DC_{pf}}\sqrt{b}/\nu_f$ (PHF case) is the Eckert number, $Nr = \frac{4\sigma^* T^3{}_\infty}{k^* k_{nf}}$ is the radiation parameter, $\beta_T = \frac{1}{b\tau_T}$ is fluid particle interaction parameter for temperature and $\gamma = \frac{C_{pf}}{C_{mf}}$ is the ratio of specific heat.

The corresponding thermal boundary conditions becomes

$$\theta(\eta) = 1 \text{ (PST case) } \theta'(0) = -1 \text{ (PHF case) at } \eta = 0,$$
$$\theta(\eta) \to 0,\ \theta_p(\eta) \to 0 \quad \text{as} \quad \eta \to \infty.$$

(3.11)

4. NUMERICAL SOLUTION

The system of coupled highly non-linear ordinary differential equations (2.9)-(2.11) and (3.9)-(3.10) subject to the boundary conditions (2.12) and (3.11) have been solved numerically using Runge-Kutta-Fehlberg (RKF45) method. This method has been successfully used by the present authors to solve various problems related to boundary layer flow and heat transfer. In this method, the edge of the boundary layer η_∞ has been chosen as $\eta = 5$, which is sufficient to achieve the far field boundary conditions asymptotically for all values of the parameters considered. A comprehensive numerical parametric computations have been carried out for various values of fluid particle interaction parameter (β), magnetic parameter (M), permeability parameter (K_P), mass concentration parameter (l), Material parameter (R), Prandtl number (Pr), Eckert number (Ec), solid volume fraction parameter (ϕ) and Radiation parameter (Nr) in both PST and PHF cases, and then the results are reported in terms of graphs.

Table 2: Values of wall temperature gradient $\theta'(0)$ for different values of the parameters.

β	M	K_p	f_0	m	R	ϕ	Nr	Ec	Pr	$f''(0)$	$\theta'(0)$	$\theta(0)$	$h'(0)$
0	0.5	0.5	0.02	0.5	1	0.2	0.5	0.2	6.2	-1.05772	-1.14999	0.88559	-0.44184
0.6										-1.11970	-1.09904	0.92407	-0.47319
1										-1.13984	-1.09157	0.92970	-0.48340
0.6	0.5	0.5	0.02	0.5	1	0.2	0.5	0.2	6.2	-1.11970	-1.09904	0.92407	-0.47319
	1									-1.19573	-1.07251	0.94389	-0.51217
	2									1.33336	-1.02385	0.98123	-0.58372
0.6	0.5	0.5	0.02	0.5	1	0.2	0.5	0.2	6.2	-1.11970	-1.09904	0.92407	-0.47319
		1								-1.24914	-1.05371	0.95817	-0.53979
		2								-1.47054	-0.97479	1.02014	-0.65619
0.6	0.5	0.5	0.02	0.5	1	0.2	0.5	0.2	6.2	-1.11970	-1.09904	0.92407	-0.47319
			0.5							-1.28671	-1.64089	0.66316	-0.64763
			1							-1.47689	-2.28985	0.50544	-0.88471
0.6	0.5	0.5	0.02	0.2	1	0.2	0.5	0.2	6.2	-1.01464	-1.13074	0.90084	0.01595
				0.5						-1.11970	-1.09904	0.92407	-0.47319
				1						-1.35425	-1.01449	0.98856	-1.54219
0.6	0.5	0.5	0.02	0.2	1	0.2	0.5	0.2	6.2	-1.11970	-1.09904	0.92407	-0.47319
					2					-0.96887	-1.14823	0.88827	-0.37026
					3					-0.86755	-1.18095	0.86517	-0.30364
0.6	0.5	0.5	0.02	0.2	1	0.05	0.5	0.2	6.2	-1.21923	-1.37483	0.77756	-0.54167
						0.1				-1.19049	-1.27307	0.82313	-0.52427
						0.2				-1.11970	-1.09904	0.92407	-0.47319
0.6	0.5	0.5	0.02	0.2	1	0.2	0.5	0.2	6.2	-1.11970	-1.09904	0.92407	-0.47319
							1			-1.11970	-0.91943	1.07502	-0.47319
							2			-1.11970	-0.47319	1.34090	-0.47319
0.6	0.5	0.5	0.02	0.2	1	0.2	0.5	0.2	6.2	-1.11970	-1.09904	0.92407	-0.47319
								0.4		-1.11970	-0.89368	1.08150	-0.47319
								0.8		-1.11970	-0.48296	1.39637	-0.47319
0.6	0.5	0.5	0.02	0.2	1	0.2	0.5	0.2	0.72	-1.11970	-0.36106	2.63493	-0.47319
									3.2	-1.11970	-0.77099	1.25799	-0.47319
									6.2	-1.11970	-1.09904	0.92407	-0.47319

5. RESULTS AND DISCUSSION

Figures 2 (a,b,c) shows the effect of suction/injection (f_0) parameter on the velocity and temperature within the boundary layer respectively. It is observed that the increase in suction/ injection parameter decreases both the velocity and temperature within the boundary layer. It is due to the fact that increasing the suction/injection parameter will slow down the flow.

The temperature profile for different values of the radiation parameter (Nr) is described as in figure 3. It is clear that, in both PST and PHF cases, the temperature increases with an increase in Nr. This is because, the large Nr values correspond to an increased dominance of conduction over radiation thereby decreasing buoyancy force and thickness of the thermal boundary layer.

Figure 4 depicts the effect of Prandtl number (Pr) on temperature distribution in PST and PHF cases. We observed that an increase in Prandtl number increases the temperature of both fluid and dust phases.

The analysis of figure 5 reveals that the effect of increasing the values of Eckert number (Ec) increases temperature distribution of both fluid and dust phase velocities in the flow region. This is due to the fact that, increasing in the values of Eckert number enhances the kinetic energy and this leads to the increase in the temperature and thermal boundary layer thickness.

Fig 6 (a,b,c) demonstrate the effects of permeability parameter (K_p) on velocity and temperature profiles. It is obvious that the presence of a porous medium causes higher restriction to the fluid flow which, in turn, slows its motion. Therefore, with increasing permeability parameter, the resistance to the fluid motion also increases. This causes the fluid velocity to decrease and due to which there is rise in temperature in the boundary layer.

To study the effects of mass concentration (l) on velocity and temperature profiles, figures (a,b,c) are plotted. From these graphs, we can observe that both profiles are decreasing functions of mass concentration.

The effect of fluid particle interaction parameter β on velocity and temperature profiles are analyzed through graphs 8 (a,b,c). It is interesting to note that, as β increases the fluidphase velocity decreases in contrast dust phase velocity increases. Whereas in temperature distribution, as expected, in both PST and PHF cases fluid phase velocity increase and dust phase velocity decreases with increasing values of β. It's because of fact that as β increases, relaxation time decreases.

The effect of magnetic parameter (M) on velocity distributions are depicted in figures 9(a). It reveals that, the increasing values of M, results in decrease of fluid and dust phase velocities. This is because of the application of a transverse magnetic field normal to the flow direction gives rise to a resistive drag-like force known as Lorentz force acting in a direction opposite to that of the flow. This has a tendency to reduce fluid transport phenomena. Therefore the momentum boundary layer thickness decreases with increasing M, hence, induces an increase in the value of the velocity gradient in both PST and PHF cases which is shown in figures 9 (b, c).

The effect of nanoparticle volume fraction parameter (ϕ) on velocity and temperature profiles for both fluid and dust phases are illustrated graphically through figures 10 (a, b, c). From these figures, it is observed that, as the volume fraction of nanoparticles increases from 0 to 0.2, velocity and temperature profiles for both fluid and dust phase increases for both the cases.

Figures 11(a,b,c) presents the velocity and temperature profiles for various values of R when $m = 0.5$. From these figures, it is observed that the velocity profile increases and the temperature profile decreases for increasing the values of R for both the phases of both PST and PHF cases.

The heat transfer characteristics of Ec with Nr and Pr with β for both PST and PHF cases are illustrated in figures 12 (a, b) and 13 (a, b) respectively. From these figures, it is observed that the Nusselt number $\theta'(0)$ decreases for PST case and increases for PHF case respectively for increasing the values of Eckert number with radiation parameter. Similarly, for increasing the

values of Prandtl number with the presence of fluid particle interaction parameter the Nusselt number increases and decreases respectively for PST and PHF cases.

The effect of angular velocity profiles on β, M, K_p, l, ϕ and R are respectively shown in figures 14, 15, 16, 17, 18 and 19. From these figures, it is observed that for increasing the values of β, M, K_p and l the angular velocity increases and decreases for increasing the values of R and ϕ.

6. CONCLUSIONS

In this paper radiation effect on Al_2O_3-water nanoparticle on micropolar fluid over a permeable stretching sheet embedded with dust particles are discussed. From this the figures, we conclude the following :

- For ϕ and R, velocity $f'(\eta)$ increases and for β, velocity decreases for fluid phase and increases for dust phase respectively as we increase the values of these parameters.
- For f_0, K_p, l, M and m, the velocity $f'(\eta)$ decreases as we go on increasing the values of these parameters.
- Temperature $\theta(\eta)$ increases for M, K_p, ϕ and m and decreases for f_0, R and l for both PST and PHF cases.
- The Nusselt number increases with increase in Eckert number, while it decreases with increasing values of Prandtl number.
- The skin friction coefficient decreases with increase in magnetic parameter, permeability parameter and coupling parameter.
- The couple stress increases with the increase the values of material parameter (R).
- Thermal boundary layer thickness decreases with increase in Prandtl number and increases with increase in Eckert number and thermal radiation for both the cases.

REFERENCES

1. B.C.Sakiadis, “Boundary layer behavior on continuous solid surfaces: I. Boundary layer equations for two dimensional and axisymmetric flow”, AIChE Journal, 7(1) (1961) 26-28.
2. F.K.Tsou, E.M.Sparrow and R.J.Goldstein, “Flow and heat transfer in the boundary layer on a continuous moving surface”, Int. J. Heat Mass Transfer, 10 (1967) 219-235.
3. L.J.Crane, “Flow past a stretching sheet”, Z. Angew. Math. Phys. (ZAMP), 21 (1970) 645-647.
4. T.Watanabe and I.Pop, “Hall effects on MHD boundary layer flow over a continuous moving flatplate”, Acta. Mech., 108 (1995) 35-47.
5. A.Chakrabarti and A.S.Gupta, “Hydromagnetic flow and heat transfer over a stretching sheet”, Quart.Appl. Math., 37 (1979) 73-78.
6. L.J.Grubka and K.M.Bobba, “Heat transfer characteristics of a continuous, stretching surface with variable temperature”, ASME J. Heat Transfer, 107 (1985) 248-250.
7. C.H.Chen, “Laminar mixed convection adjacent to vertical, continuously stretching sheets”, Heat and Mass Transf., 33 (1998) 471-476.
8. M.S.Abel and N.Mahesha, “Heat transfer in MHD viscoelastic fluid flow over a stretching sheet with variable thermal conductivity, non-uniform heat source and radiation”, Appl. Math. Model, 32 (2008)1965-1983.
9. B.K.Dutta, P.Roy and A.S.Gupta, “Temperature field in flow over a stretching sheet with uniform heatflux”, International Communications in Heat and Mass Transfer, 12(1) (1985) 89-94.
10. M.E.Ali, “Heat transfer characteristics of a continuous stretching surface”, Heat and Mass Transfer,29(4) (1994) 227234.
11. K.Vajravelu and T.Roper, “Flow and heat transfer in a second grade fluid over a stretching sheet”, Int.J. Non-linear Mechanics, 34(6) (1999) 1031-1036.
12. A.C.Eringen, “Theory of micropolar fluids”, Journal of Mathematics and Mechanics, 16 (1966) 1-18.
13. J.Peddison and R.P.McNitt, “Boundary layer theory for micropolar fluid”, Recent Advances in Engineering Science, 5 (1970) 405-426.
14. RoslindaNazara, Norsarahaida Amina, Diana Filip and Ioan Pop, “Stagnation point flow of

a micropolar fluid towards a stretching sheet", International Journal of Non-Linear Mechanics, 39 (2004)1227-1235.
15. M.M.Rahman and M.A.Sattar 'Convective heat transfer flow of a micropolar fluid past a continuously moving vertical porous plate with time dependent suction in the presence of radiation", Int. J. Appl.Mech. Eng., 12 (2007) 497.
16. A.Raptis, "Flow of micropolar fluid past a continuously moving plate by presence of radiation", International journal of Heat and Mass Transfer, 41 (1998) 2865-2866.
17. Anura Ishak, "Thermal boundary layer flow over a stretching sheet in a micropolar fluid with radiation effect", Meccannica, 45 (2010) 367-374.
18. M.Turkyilmazoglu, Flow of a micropolar fluid due to a porous stretching sheet and heat transfer, International Journal of Non-Linear Mechanics, 83 (2016) 59-64.
19. W.Ibrahim, MHD boundary layer flow and heat transfer of micropolar fluid past a stretching sheet with second order slip, Journal of the Brazilian Society of Mechanical Sciences and Engineering, 39 (3) (2017) 791–799.
20. S.U.S.Choi, "Enhancing thermal conductivity of fluids with nanoparticles", ASME Fluids Engineering Division, 231 (1995) 99-105.
21. H.Masuda, A.Ebata, K.Teramae and N.Hishinuma, Alteration of thermal conductivity and viscosity of liquid by dispersing ultra-fine particles, Netsu Bussei., 7 (1993) 227-233.
22. J.Buongiorno, Convective transport in nanofluids, ASME J. Heat Transfer, 128 (2005) 240-250.
23. YiminiXuon and Qiang Li, 'Heat transfer enhancement of nanofluids", International Journal of Heat and Fluid flow, 21(1) (2000) 58-64.
24. Sarit Kumar Das, Nandy Putra, Peter Thiesen and Wilfried Roetzel, 'Temperature dependence of thermal conductivity enhancement for nanofluids", J. Heat Transfer, 125(4) (2003) 567-574.
25. M.M.Rashidi, N.Vishnu Ganesh, A.K.Abdul Hakeem and B.Ganga, "Buoyancy effect on MHD flow of nanofluid over a stretching sheet in the presence of thermal radiation", Journal of Molecular Liquids,198 (2014) 234-238.
26. G. Madaki, R. Roslan, R. Kandasamy, and M. S. H. Chowdhury, Flow and heat transfer of nanofluid over a stretching sheet with non-linear velocity in the presence of thermal radiation and chemical reaction, AIP Conference Proceedings **1830**, 020014 (2017.
27. B.C.Prasannakumara, M.R.Krishnamurthy, B.J.Gireesha and Rama S.R.Gorla, "Effect of Multiple Slips and Thermal Radiation on MHD Flow of Jeffery Nanofluid with Heat Transfer", Journal of Nanofluids, 5(2016) 1–12,
28. P.G.Saffman, "On the stability of laminar flow of a dusty gas", J. fluid Mech., 13 (1962) 120-128.
29. K.M.Chakrabarti, "Note on Boundary layer in a dusty gas", AIAA J., 128 (1974) 136-137.
30. N.Datta and S.K.Mishra, "Boundary layer flow of a dusty fluid over a semi infinite flat plate", Act.Mech., 42 (1982) 71-73.
31. Evgeny S Asmolov and Sergsi V Manuilovich, "Stability of a dusty gas laminar boundary layer on a flat plate", J. Fluid Mechanics, 365 (1998) 137-170.
32. K.Vajravelu and J.Nayfeh, "Hydromagnetic flow of a dusty fluid over a stretching sheet", Int. J. Nonlin.Mech., 27 (1998) 937-945.
33. M.A.Ezzat, "State space approach to solids and fluids", Canadian Journal of Physics, 86(11) (2008)1241-1250.
34. M. R. Krishnamurthy, B. J. Gireesha, Rama Subba Reddy Gorla and B. C. Prasannakumara, Suspended Particle Effect on Slip Flow and Melting Heat Transfer of Nanofluid Over a Stretching Sheet Embedded in a Porous Medium in the Presence of Nonlinear Thermal Radiation, Journal of Nanofluids, 5 (2016) 1–9.
35. G.Ahmadi, "Self-similar solution of incompressible micropolar boundary layer flow over a semi-infinite flat plate", Int. J. Eng. Sci., 14 (1976) 639–646.
36. H.C.Brickman, "The viscosity of concentrated suspensions and solution", J. Chem. Phys., 20(1952) 571–81.

37. J.Maxwell, "A Treatise on Electricity and Magnetism". 2nd ed., Oxford University Press, Cambridge, UK (1904).

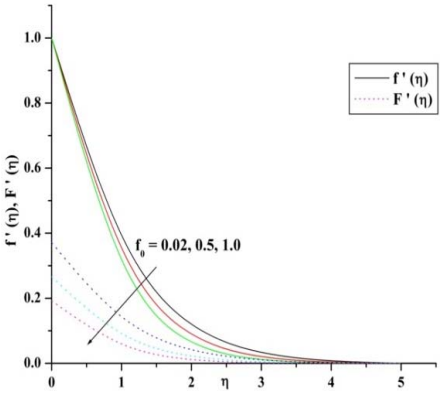

Figure 2(a):Effect of f_0 on velocity profile.

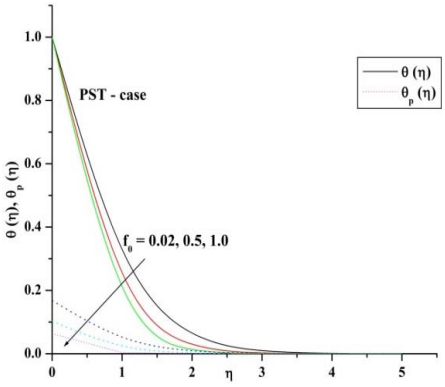

Figure 2(b): Effect of f_0 on temperature profile for PST case.

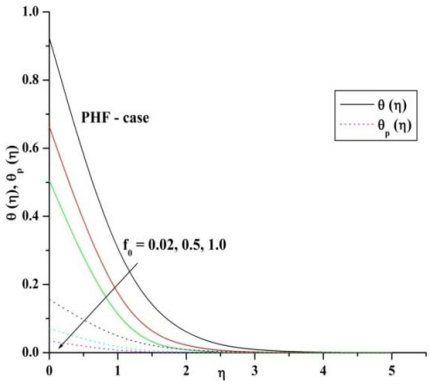

Figure 2(c):Effect f_0 on temperature profile for PHF case.

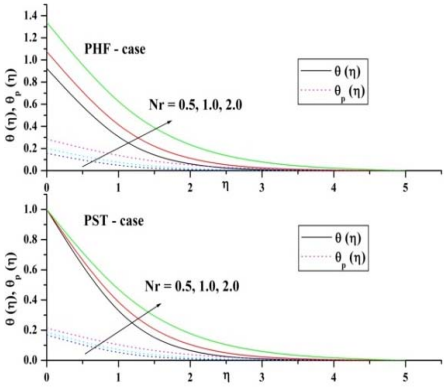

Figure 3: Effect of Nr on temperature profiles for both PST and PHF

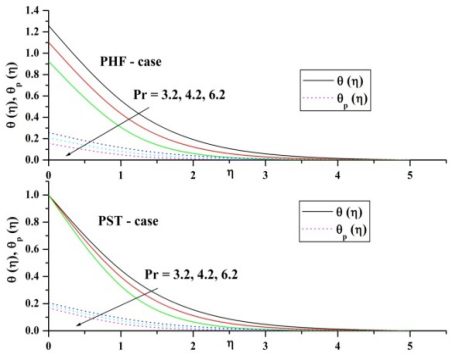

Figure 4: Effect of Pr on temperature profiles

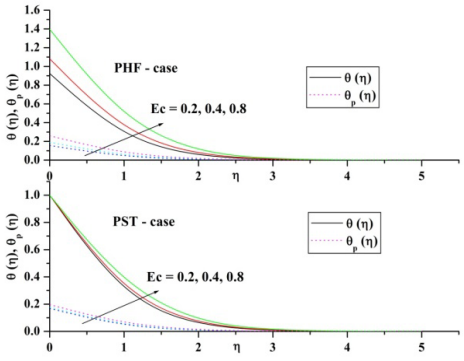

Figure 5: Effect of Ec on temperature profile for both PST and PHF case.

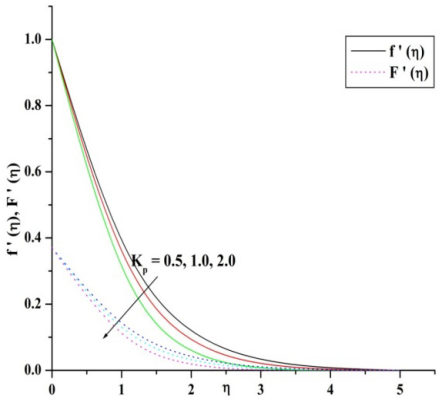

Figure 6(a): Effect of $K_p$on velocity profile

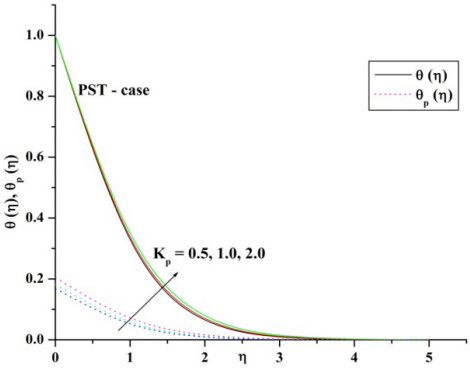

Figure 6(b): Effect of $K_p$on temperature profile for PST case.

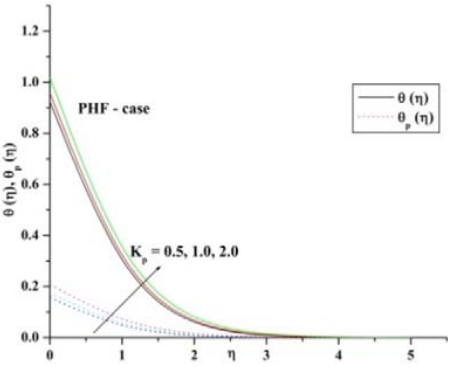

Figure 6(c): Effect of K_p on temperature profile

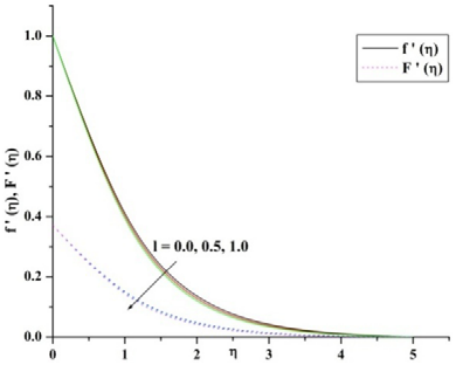

Figure 7(a): Effect of l on velocity profiles. for PHF case.

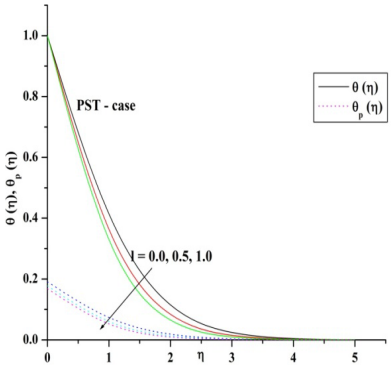

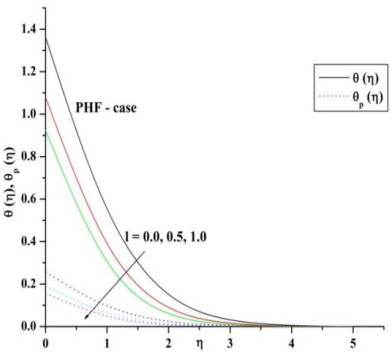

Figure 7(b)& 7(c): Effect of l on temperature profile for PST and PHF cases.

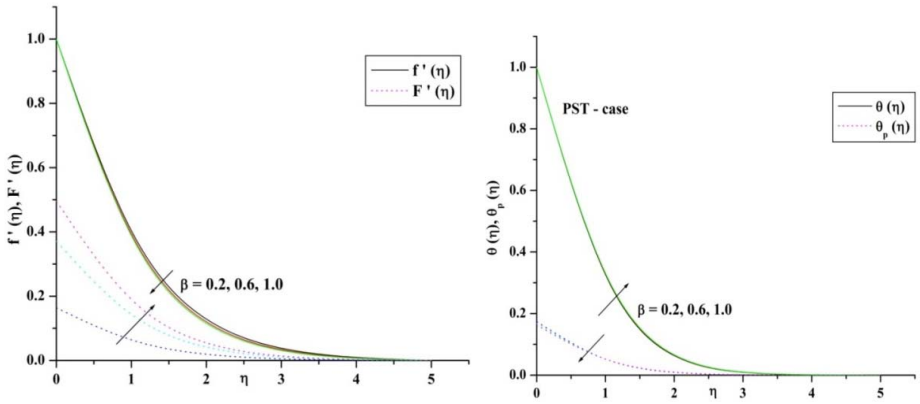

Figure 8(a): Effect of β on velocity profile. Figure 8(b): Effect of β on temperature profile for PST case.

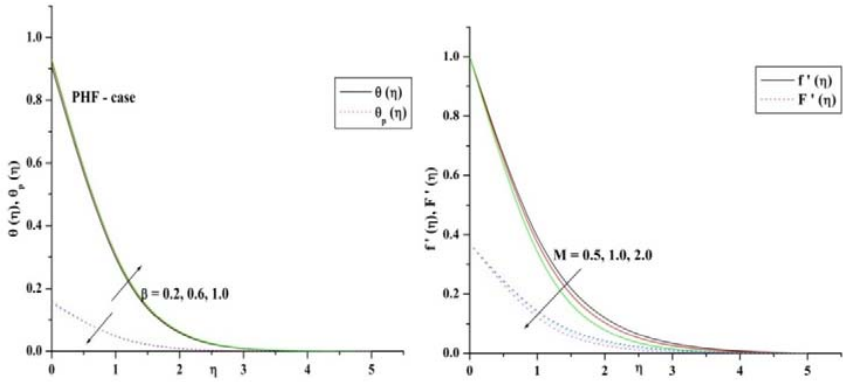

Figure 8(c): Effect of β on temperature profile for PHF case Figure 9(a): Effect of M on velocity profile.

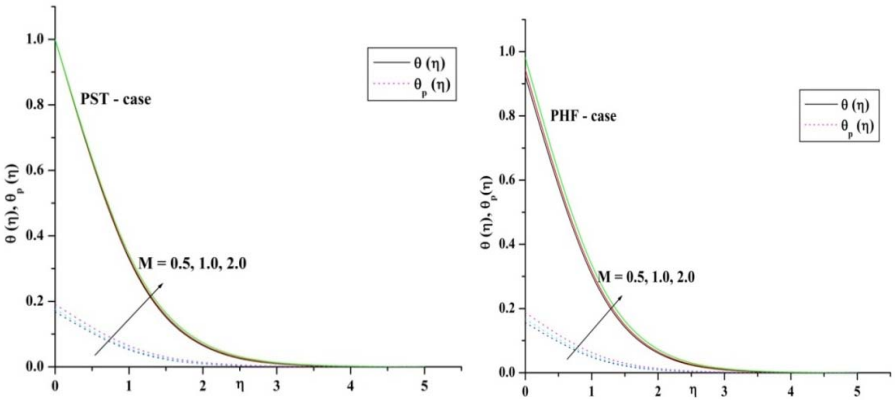

Figure 9(b) & 9(c): Effect of M on temperature profile PST & PHF case.

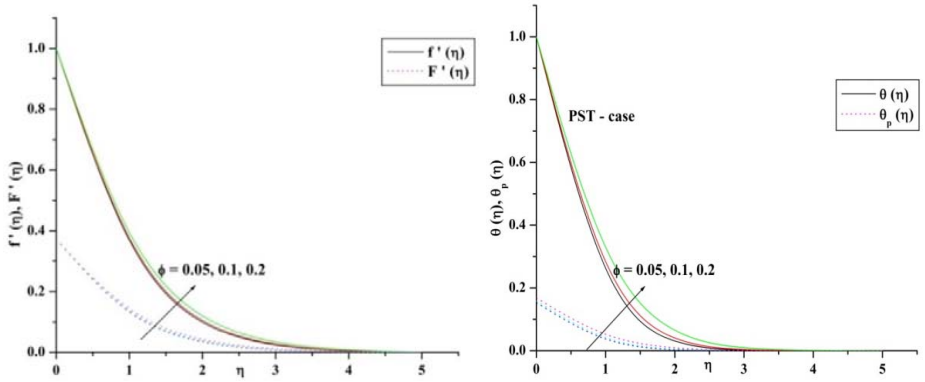

Figure 10(a): Effect of ϕ on velocity profiles. Figure 10(b): Effect of ϕ on temperature profile for PST case.

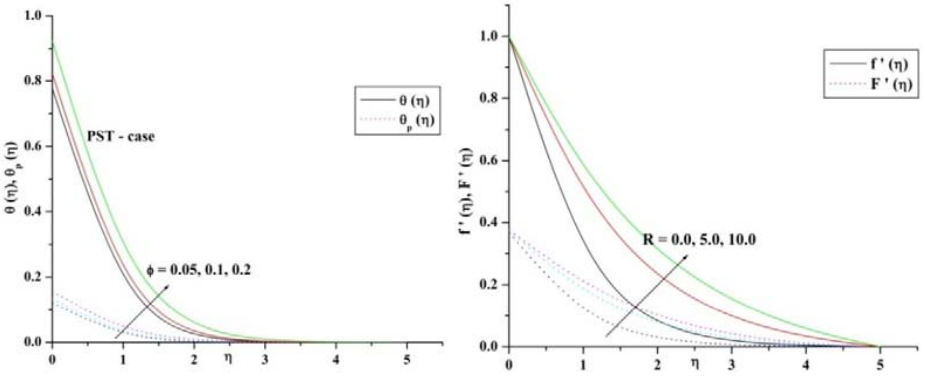

Figure 10(c): Effect of ϕ on temperature profile for PHF case. Figure 11(a): Effect of R on velocity profile.

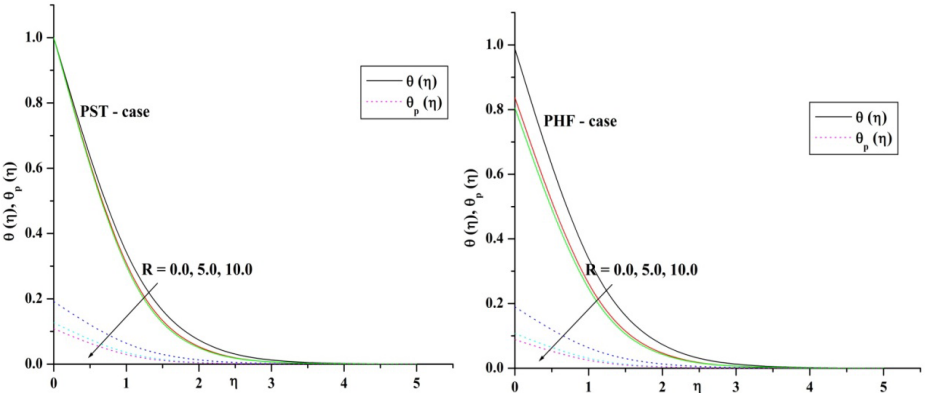

Figure 11(b) & 11(c): Effect of R on temperature profile for PST and PHF cases.

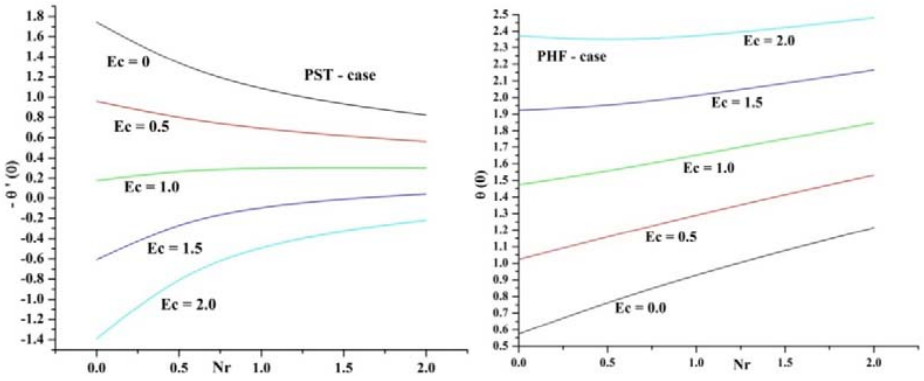

Figure 12(a) & 12 (b): Heat transfer characteristics for different values of Ec and Nr for PST and PHF cases.

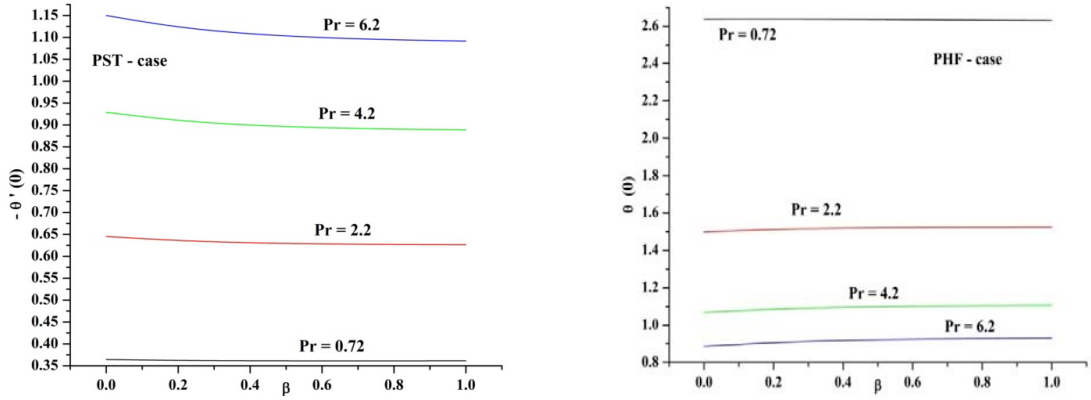

Figure 13(a) & 13 (b): Heat transfer characteristics for different values of Pr and β for PST and PHF cases.

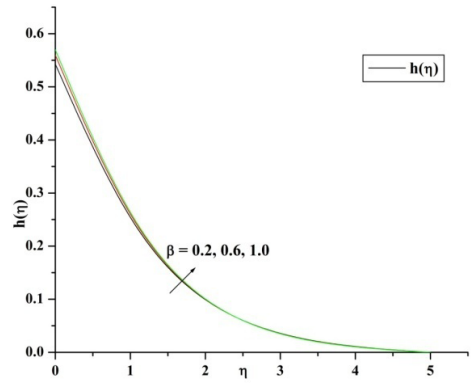

Figure 14: Effect of β on angular velocity

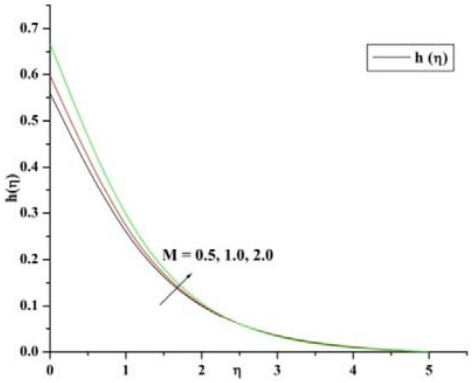

Figure 15: Effect of M on angular velocity profile

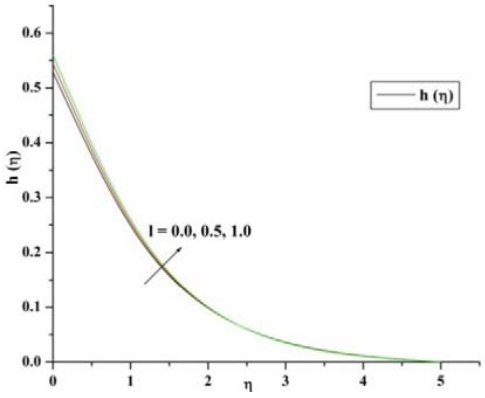

Figure 16: Effect of l on angular velocity profile.

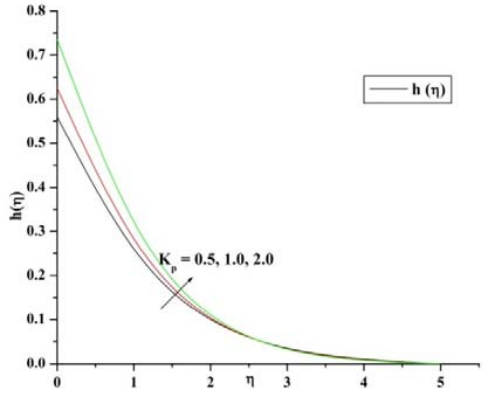

Figure 17: Effect of K_p on angular velocity profile.

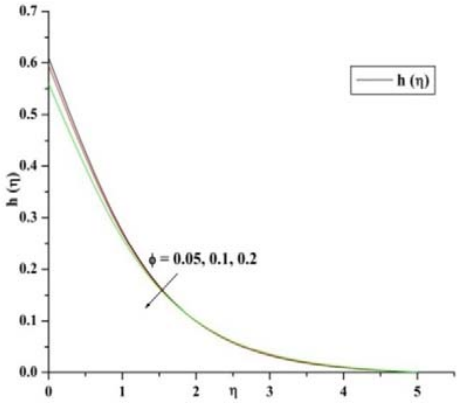

Figure 18: Effect of ϕ on angular velocity profile.

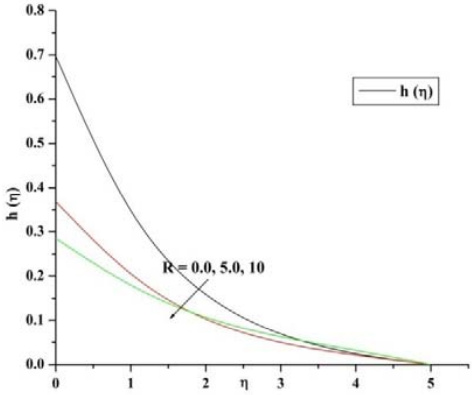

Figure 19: Effect of R on angular velocity profile.

***